

LATERAL VELOCITY ESTIMATION FROM UNSTACKED DATA

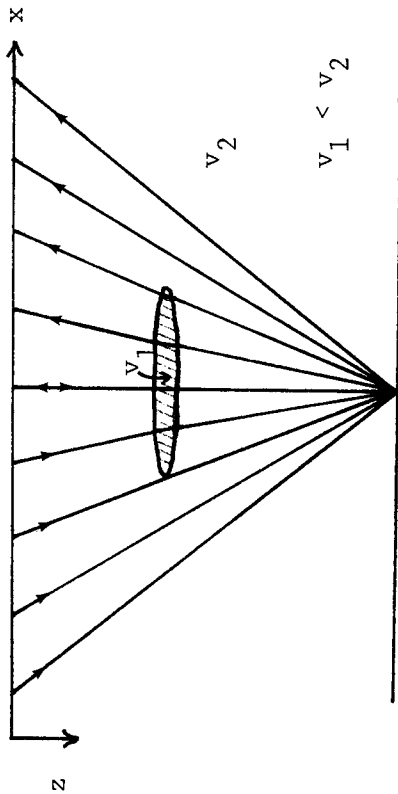
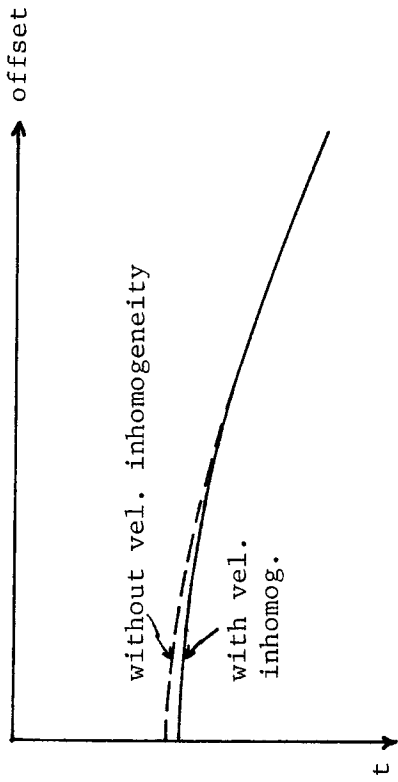
Walt Lynn

Introduction

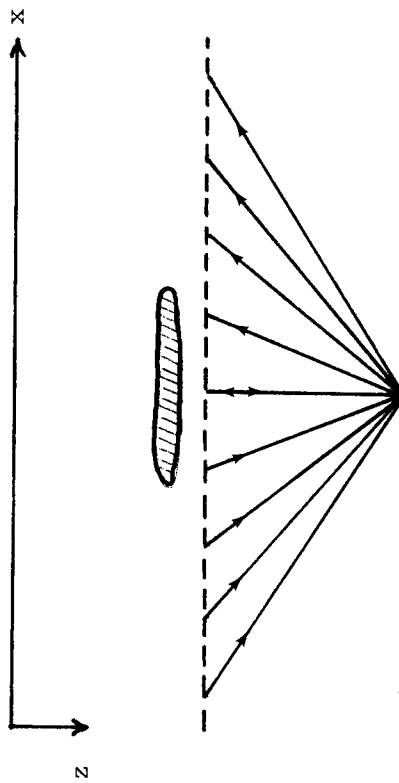
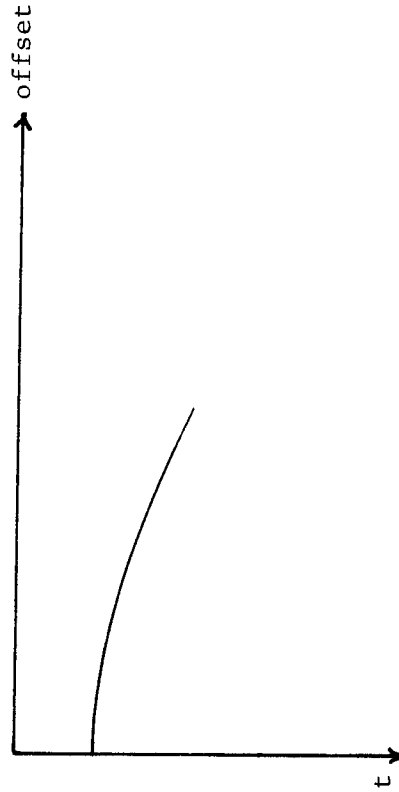
In the presence of strong lateral velocity variations, velocity estimations based on surface data are often incorrect or of low quality. A more accurate velocity estimation can be made at some depth by basing the velocity estimate on the data that would be produced and recorded near that depth. These data can be simulated by downward continuing the common shot and common geophone gathers to some datum level and thus removing the effects of any known or estimated lateral velocity variations above this level. In this paper, we will present the background and motivation for such a method of velocity estimation based on the downward continuation of unstacked data, i.e., common shot and common geophone gathers.

One type of problem in estimating velocity in a laterally varying medium with CMP gathers is illustrated in Fig. 1. Shown is a low-velocity lens embedded in the upper layer of a two-layer medium. The lateral extent of the lens is roughly one-third that of the maximum offset. For the CMP gather whose midpoint is centered over the lens, the velocity below the lens to the plane reflector will appear faster because of the decrease in moveout on the near offsets. Ideally, we would like to measure the velocity below the lens using the setup in Fig. 1(b) so that the effect of the lens is removed. Because CMP gathers are not true wavefields,* however, there is no way we can create the experiment in Fig. 1(b) by downward continuing the surface CMP gathers (common offset gathers won't work either). To create the experiment in Fig. 1(b), we must downward continue the true wavefield common shot and common geophone gathers and reorganize the data into CMP gathers. Such a procedure is

*We use the term true wavefield to mean a wavefield that can be reproduced by a single experiment consisting of one receiver distribution recording the energy from one source distribution.



a. velocity estimate based on surface data



b. velocity estimate based on data shot and recorded below the inhomogeneity

FIGURE 1.—One type of problem in estimating velocity from surface data in the presence of lateral velocity variations. Velocity is estimated by measuring a coherency along hyperbolas in (offset,t) space for various velocities in the CMP gathers. The velocity of the lens is slower than that of the surrounding medium causing a travel time delay on the inner traces of the surface data for the event shown (upper plot). Consequently, the velocity determined for this event will be incorrect. A more desirable experiment would be the one shown in the lower left-hand drawing where the lens has no effect on the velocity estimate. Such an experiment can only be simulated by downward continuing real wavefields. Common midpoint and common offset sections *cannot* be downward continued to simulate this experiment.

cumbersome and therefore we are motivated to develop a velocity estimation procedure based on the common shot and common geophone gathers themselves without having to reorganize the data at each depth into CMP gathers.

An integral part of velocity estimation using unstacked data is the use of the 15° approximation to the wave equation as the downward continuing operator, since this equation can be made velocity independent by a simple change of coordinates (this will be shown later). The advantage in doing this is that the data can be migrated immediately after the velocity estimation by simply transforming the wavefield back into the real earth coordinates. This eliminates an additional step of starting over and redoing the downward continuation with the correct velocity to get the downward-continued wavefield, as is the case with bootstrapping velocity estimation methods. Unfortunately, the range of propagation angles in common shot and geophone gathers usually exceeds the accuracy limitations of the 15° equation. We will show that alleviating this problem leads to the use of slanted coordinates.

Before discussing velocity estimation using the unstacked downward continued field gathers, we will first outline the method of plane-wave stacks (p-stacks) using stacked downward continued data since it has only been presented orally (Schultz and Claerbout [1]). Following this, we will show (1) how to estimate velocity using unmoved-out downward-continued data (assuming, incorrectly, the 15° approximation is valid), and then (2) how it is to be applied to linearly-moved-out data (where the 15° approximation is valid).

Velocity Estimation Using Plane-Wave Stacks

What follows is only a terse description of velocity estimation using plane wave stacks and is intended to fill in a gap in the SEP reports. For greater detail, the reader is referred to Schultz's thesis [2].

The central idea of plane wave stacks is to synthesize a downgoing plane wave from common shot or common geophone gathers (depending on the desired angle of propagation of the plane wave), where each plane wave is characterized by a ray parameter $p = \sin\theta/v$. Invoking reciprocity we can always interchange the shot and receiver positions, and so, in the case of a common shot gather, to simulate a plane wave traveling from the geophones back to the source, we simply apply a linear moveout to the common shot traces and superimpose them [see Figs. 2(a), (b)]. The linear moveout applies only if the near surface velocity is constant; otherwise some other summation trajectory will apply. The resultant

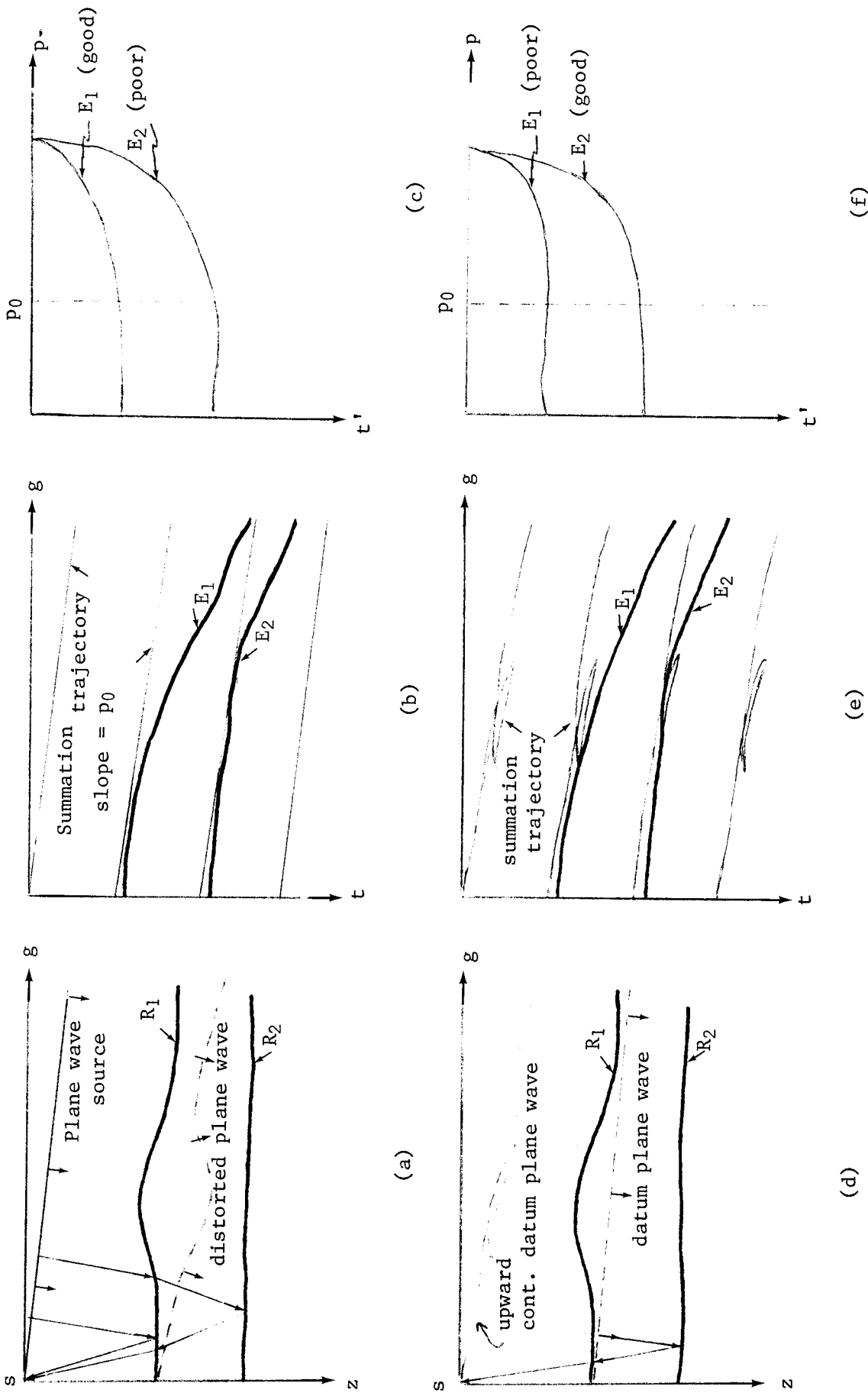


FIGURE 2.—Diagram showing the steps involved in plane-wave stack velocity estimation. The structure shown in (a) and (d) consists of two reflectors R_1 and R_2 corresponding to the events E_1 and E_2 in (b) and (e). (a) Desired plane-wave source is created from a common shot gather for a particular ray parameter $p_0 (= \sin\theta/v)$. The plane becomes distorted after passing through the first reflector R_1 , thus causing a deterioration in the velocity estimate below R_1 . (b) To simulate the plane wave shown in (a) from the common-shot gather, the roles of shot and geophones are interchanged using reciprocity and the amplitudes are summed along the straight lines (slope = p_0). The resultant summation represents the seismic trace recorded if the source were a plane wave with a ray parameter p_0 . (c) p-gather formed from several plane wave summations like (b). Hyperbolic events in x, t space map into ellipses in p, t' space. Root-mean-square velocity is estimated by measuring a coherency along the ellipse for different velocities. A good coherency is measured for the event E_1 because it is illuminated by a true plane wave. On the other hand, a poor coherency is measured for event E_2 because of distortion of the illuminating plane wave. (d), (e), and (f) are the same as (a), (b), and (c),

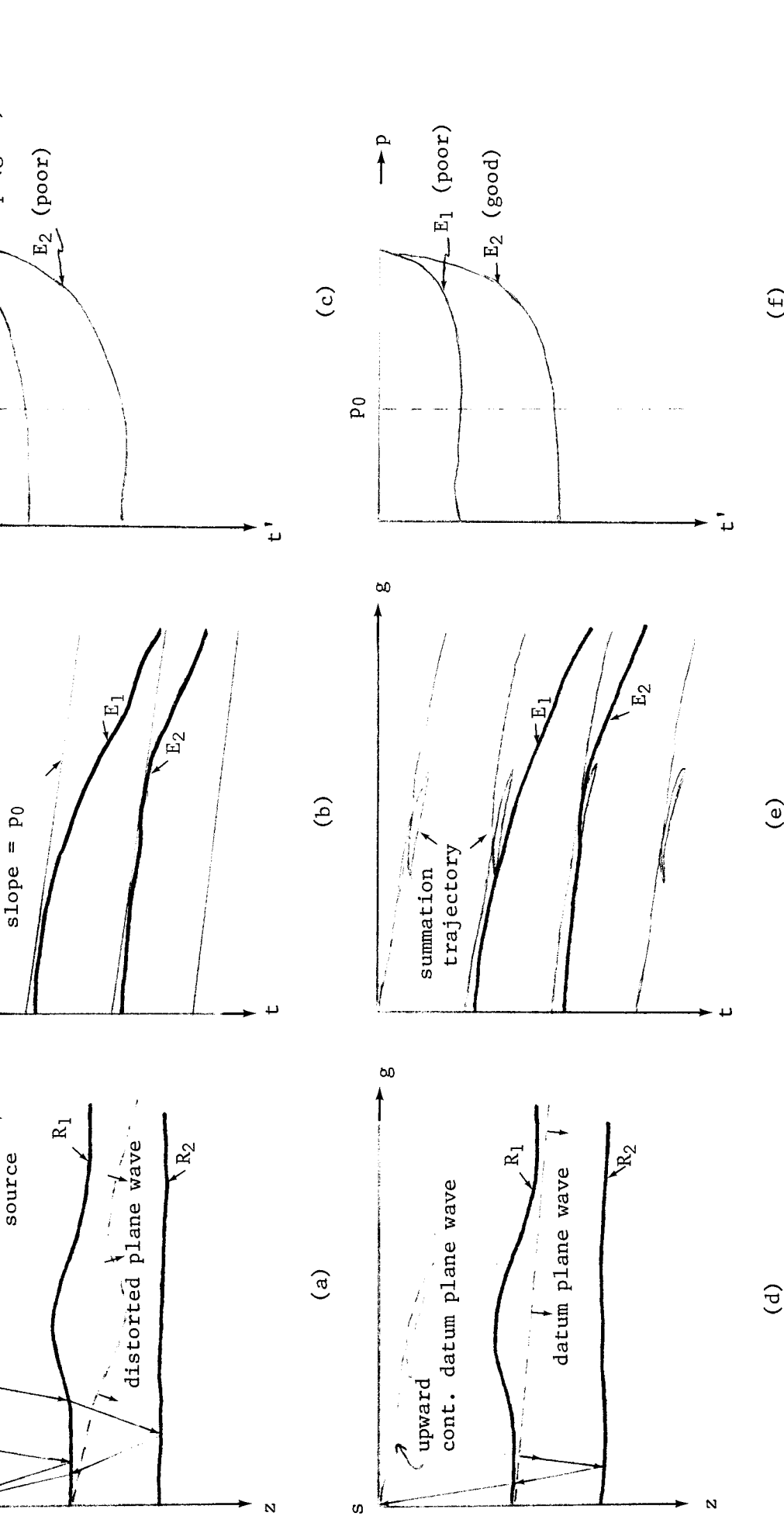


FIGURE 2.—Diagram showing the steps involved in plane-wave stack velocity estimation. The structure shown in (a) and (d) consists of two reflectors R_1 and R_2 corresponding to the events E_1 and E_2 in (b) and (e). (a) Desired plane-wave source is created from a common shot gather for a particular ray parameter p_0 ($= \sin\theta/v$). The plane becomes distorted after passing through the first reflector R_1 , thus causing a deterioration in the velocity estimate below R_1 . (b) To simulate the plane wave shown in (a) from the common-shot gather, the roles of shot and geophones are interchanged using reciprocity and the amplitudes are summed along the straight lines (slope = p_0). The resultant summation represents the seismic trace recorded if the source were a plane wave with a ray parameter p_0 . (c) p-gather formed from several plane wave summations like (b). Hyperbolic events in the x, t space map into ellipses in p, t' space. Root-mean-square velocity is estimated by measuring the ellipse for different velocities. A good coherency is measured for the event E_1 because it is illuminated by a true plane wave. On the other hand, a poor coherency is measured for event E_2 because of distortion of the illuminating plane wave. (d), (e), and (f) are the same as (a), (b), and (c), except now the source is a true plane wave below R_1 . The summation trajectories are determined by upward continuing datum plane waves for a range of p values. The velocity estimate for the event E_2 is superior to that measured using the surface data. More details are given in the text.

trace approximates a seismogram recorded as if the actual source were a plane wave, with a ray parameter p_0 and becomes one member of a p-gather [Fig. 2(c)]. The other members of the p-gather are found by synthesizing many different plane waves all of which are characterized by a unique ray parameter p . When these stacked traces are displayed side by side for linearly increasing values of p , it turns out that a hyperbolic event in (x,t) space becomes an ellipsoidal event in (p,t') space. The shape of the ellipse depends directly on rms velocity, so the rms velocity to the event can be estimated by calculating a coherency or semblance along the ellipse for different velocities in much the same manner as it is calculated for hyperbolic events.

The quality of the velocity estimate is directly related to the quality of the plane wave. If the medium contains lateral velocity variations, the initial plane wave becomes distorted and any velocity estimations based on this source are consequently deteriorated. To obtain accurate velocity estimates at depth, it is therefore desirable to resum the common shot gathers along a trajectory that will simulate a plane wave at the desired depth. To do so, we use the velocity estimates from all p-gathers down to some level z_0 and propagate the desired datum plane wave back up to the surface [see Fig. 2(d)]. The shape of the wavefront at the surface determines the summation trajectory needed to create the desired plane wave at z_0 [Fig. 2(e)]. However, because of known or estimated lateral velocity variations, the summation trajectory needed to create a plane wave at the required depth will in general no longer be a straight line (for more details, see refs. [2] and [4]). After the velocity has been estimated for all gathers, a new set of datum plane waves is simulated at still greater depths by using the velocity estimates of the previous steps, and the entire procedure is repeated until the whole section is processed.

Using p-stacks to estimate velocity in a laterally varying medium is theoretically sound but has the undesirable quality of being cumbersome in practice. At each level, a new p-gather must be created by generating the necessary summation trajectories for each common-shot (or common geophone) gather. Migration is accomplished by downward continuing both shots and geophones, but this can be accomplished only after the velocity has been estimated. We are thus motivated to develop a velocity estimation procedure which deals with the unstacked downward continued shot and geophone gathers directly and allows us to estimate velocity and migrate the data at the same time.

Velocity Estimation with Unstacked, Unmoved-out Data

Consider for the moment a common shot gather whose cable length is short enough so the impinging recorded energy travels along rays within 15° to the vertical. We will later relax this restriction when we transform the data to a slanted coordinate system, but for now we will keep it to illustrate how we can use downward-continued data to estimate velocity.

In a retarded time frame for upcoming waves ($t' = t + \int_0^z dz/v$), the full wave equation becomes

$$Q_{x'x'} + Q_{z'z'} + (2/v)Q_{z't'} = 0, \quad (1)$$

where Q is the wavefield described in the primed coordinate system, and x' is the geophone or shot location (depending on whether the gather is a common shot or a common geophone one). If the 15° approximation is valid, then the $Q_{z'z'}$ term may be omitted, leaving the well-known 15° equation:

$$Q_{z't'} = -(v/2)Q_{x'x'}. \quad (2)$$

Defining a new coordinate,

$$d' = \int_0^z v dz, \quad (3)$$

and changing variables from z' to d' , makes Eq. (2) velocity independent.

$$Q_{d't'} = -\frac{1}{2} Q_{x'x'}. \quad (4)$$

Since the transformation of the surface data requires no information about velocity ($\int_0^0 dz/v = 0$), we can use Eq. (4) as our operator to downward continue both the shots and geophones. After we estimate velocity (shown next), a simple coordinate transformation back to real earth coordinates produces a migrated gather.

The velocity is estimated by measuring the values of d' at which the events focus and the top of the hyperbola t_0' :

$$d_0 = \int_0^{z_0} v dz, \quad (5)$$

$$t_0' = \int_0^{z_0} \frac{dz}{v}. \quad (6)$$

Combining (5) and (6) yields directly a measure of the rms velocity to a particular event:

$$v_{\text{rms}}^2 = \frac{1}{t_0'} \int_0^{t_0'} v^2 dt = \frac{d_0'}{t_0'} . \quad (7)$$

Unfortunately, the 15° equation is not an accurate operator to use on unmoved-out field data because the propagation angles vary substantially beyond 15° from the vertical. Consequently, it is necessary to keep the Q_{zz} derivative in Eq. (1), which can be approximated from (2) as

$$Q_{z'z'} = -\frac{v}{2} Q_{x'x'z'}^{t'} , \quad (8)$$

where the t -superscript denotes a time integration. Substitution of (8) into (1) gives the so-called 45° approximation:

$$Q_{t'z'} = -\frac{v}{2} Q_{x'x'} + \frac{v^2}{4} Q_{x'x'z'}^{t'} . \quad (9)$$

Equation (9), however, cannot be made velocity independent like the 15° equation (2). Hence, any velocity estimation scheme using downward continued data with the 45° equation (or better) must be an iterative one. That is, an initial velocity function must be estimated and the data migrated using that estimate. Depending on the amount of over- or undermigration of particular events, the old velocity estimate can be improved. The migration can be repeated with new velocity estimates until all events focus as well as possible. Such a procedure is also cumbersome, but for unmoved-out field data there is no apparent alternative.

Downward Continuation of Linearly Moved-Out Data

The range of propagation angles for common shot and common geophone gathers is usually centered around some non-zero angle to the vertical. If, instead of downward continuing the gathers straight down, we downward continue them along some average incident angle [compare Figs. 4(b) and 5(b)], then it becomes possible to use the 15° equation as our wave propagator. Moreover, we can then take advantage of a transformation similar to Eq. (3) that makes the

wave equation velocity independent. We will see shortly that the result of a slanted downward continuation is to make the energy migrate not to the top of some hyperbola, but to some point on its flank. In a linearly moved-out coordinate system, this point becomes the top of a skewed hyperbola.

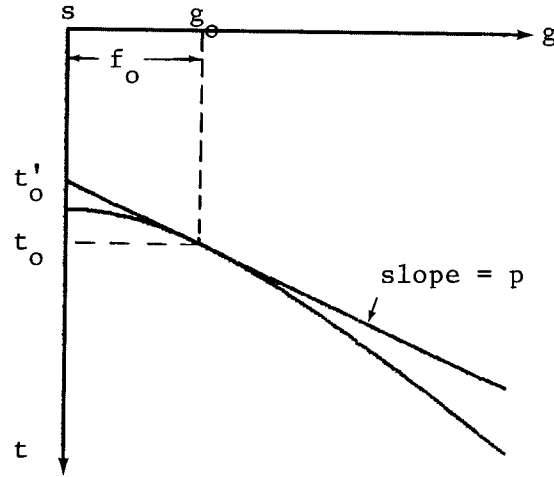
In this section, we will first demonstrate how to estimate velocity using the location of the point on the hyperbola flank. Secondly, we will demonstrate that since energy does not have to migrate as far, downward continuation of linearly moved-out data is less sensitive to velocity errors.

Figure 3(a) shows a hyperbolic event recorded at the surface due to a plane layer at $z_0 = v t_0$. If we fix a slope p (which is a ray parameter) to a line in (x,t) space and slide the line down until it is tangent to the hyperbola at some f_0, t_0 ($f_0 = \text{offset}$), then the rms velocity along the ray path from the shot s to the geophone at g_0 is given by

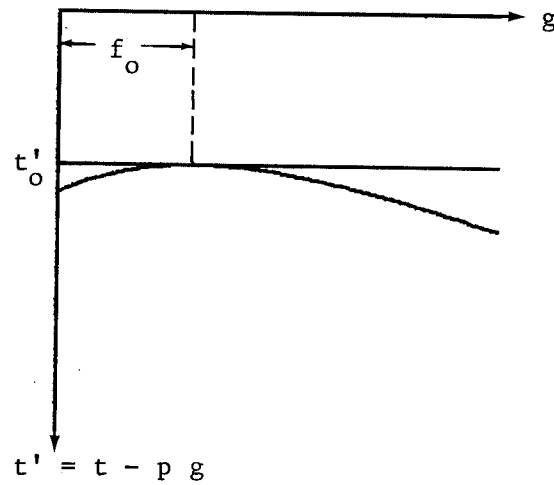
$$v_{\text{rms}}^2 = \frac{f_0/t_0'}{p[1 + p(f_0/t_0')]} , \quad (10)$$

where $t_0' = t_0 - p f_0$. This result is derived by Claerbout [3]. A velocity estimate can be directly made on the parameters p , f_0 , and t_0' , without any need for measuring curvature. Consider now applying a linear moveout, $t' = t - p_0 f$, to the gather in Fig. 3(a). The effect of this moveout is to make the tangency point the top of some hyperboloid and the problem of estimating velocity becomes one of locating this top [see Fig. 3(b)]. As we want to consider velocity estimation in a laterally varying medium, it is necessary to perform the velocity estimation on downward-continued data as opposed to surface data. If we migrate the linearly moved-out gather in Fig. 3(b), the problem of estimating a tangency point becomes one of estimating a focus. The downward continuation in the linearly moved-out coordinate system is equivalent to pushing the geophones down at some non-zero angle to the vertical. This has several advantages over the vertical downward continuation that we will now discuss.

Figure 4(b) illustrates how energy emanating from a point migrates as the geophones are pushed straight downward. The hyperbola branches in Fig. 4(a) show the corresponding travel time hyperbolas recorded at the different depths. As the geophone depth approaches the depth of the point scatterer, the energy migrates toward the receiver directly over the scatterer. If the correct velocity is used, the geophones are downward continued to the correct depth and the hyperbola collapses



a



b

FIGURE 3.—Velocity estimation without measuring curvature. (a) Rms velocity from s to g_0 can be directly measured from the parameters t_0' , f_0 , and p by Eq. (10). (b) Effect of a linear moveout on the hyperbola. Point of tangency is now the top of the skewed hyperbola. The problem of finding tangency points now becomes one of finding hyperbola tops, an operation perfectly suited for migration. See reference [2] for the development of this method.

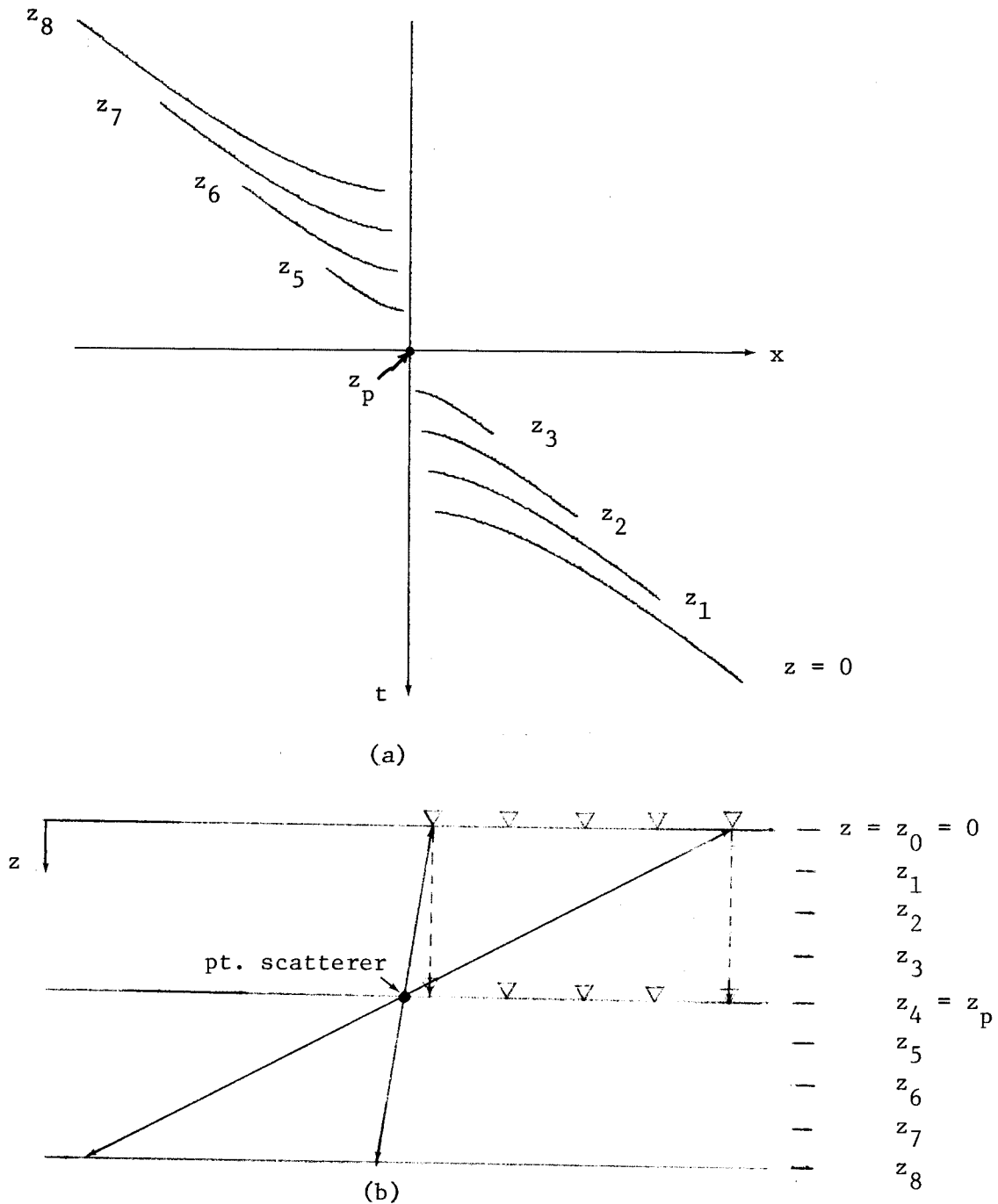


FIGURE 4.—Vertical downward continuation of receivers. (a) Travel time curves from a point scatterer at $z = z_p$ to receivers at different z levels. As the receiver level approaches the point scatterer level, energy migrates toward the zero offset trace. If the receivers are pushed down too far, by overestimating velocity, the energy migrates through the focus and forms the inverted hyperbola branches in the upper left-hand quadrant. The large deviation of propagation angles precludes the use of the 15° equation as the downward continuation operator. The hyperbola branches are plotted vs. retarded in Fig. 6(a).

to a focus at the receiver directly over the scatterer. If too high a velocity is used, the receivers are downward continued too far and the energy migrates through the focus and outside of the gather, forming the inverted hyperbolas in the upper left-hand quadrant. Hence, the lower right-hand quadrant in Fig. 4(a) represents undermigrated energy and the upper left quadrant represents overmigrated energy.

Consider now the situation where the geophones are downward continued along some slanted path to the vertical [Fig. 5(b)], and for the moment assume a constant velocity medium. Each geophone is pushed down along a straight line of constant x' , where

$$x' = x + z \tan\theta.$$

Figure 5(a) shows how the hyperbolas collapse to a point as the geophones are pushed down toward the point scatterer. Only now the energy migrates to a point on the flank of the original surface recorded hyperbola [shown by dashed line in Fig. 5(a)] corresponding to the receiver at x_0' . This is the situation we want to estimate velocity using the scheme shown in Fig. 3. If the receivers are pushed down too far, because of overestimating velocity, the energy again migrates through a focus forming the inverted hyperbolas in the upper right quadrant. The overmigrated energy in this case, however, has not migrated off the gather as in the case of vertical downward continuation.

It is important to note that since the hyperbola is collapsing to some point on its flank, the energy does not have to migrate as far to get there. Instead of migrating to the inner traces when downward continuing vertically, the energy is now migrating from both the inner and outer traces towards some intermediate trace. Intuitively then, the downward continuation should be less sensitive to velocity variations or errors. We also note that energy is migrating to a point which actually exists on the surface data, whereas in the case of the vertical downward continuation, it is not if the zero offset trace is missing (as it usually is in marine data).

Figure 6 illustrates the concepts of Figs. 4 and 5 in the retarded time frames used in the migration of upcoming waves. Figures 6(a) and (b) correspond to vertical and slanted downward continuation and are the same as Figs. 4(a) and 5(a), respectively, but the depth dependent time shift has moved all of the hyperbolas so they are tangent at the focus point. The time shift for the data in 6(a) is the well-known upgoing wave transformation, $t' = t + z/v$ and in 6(b) is

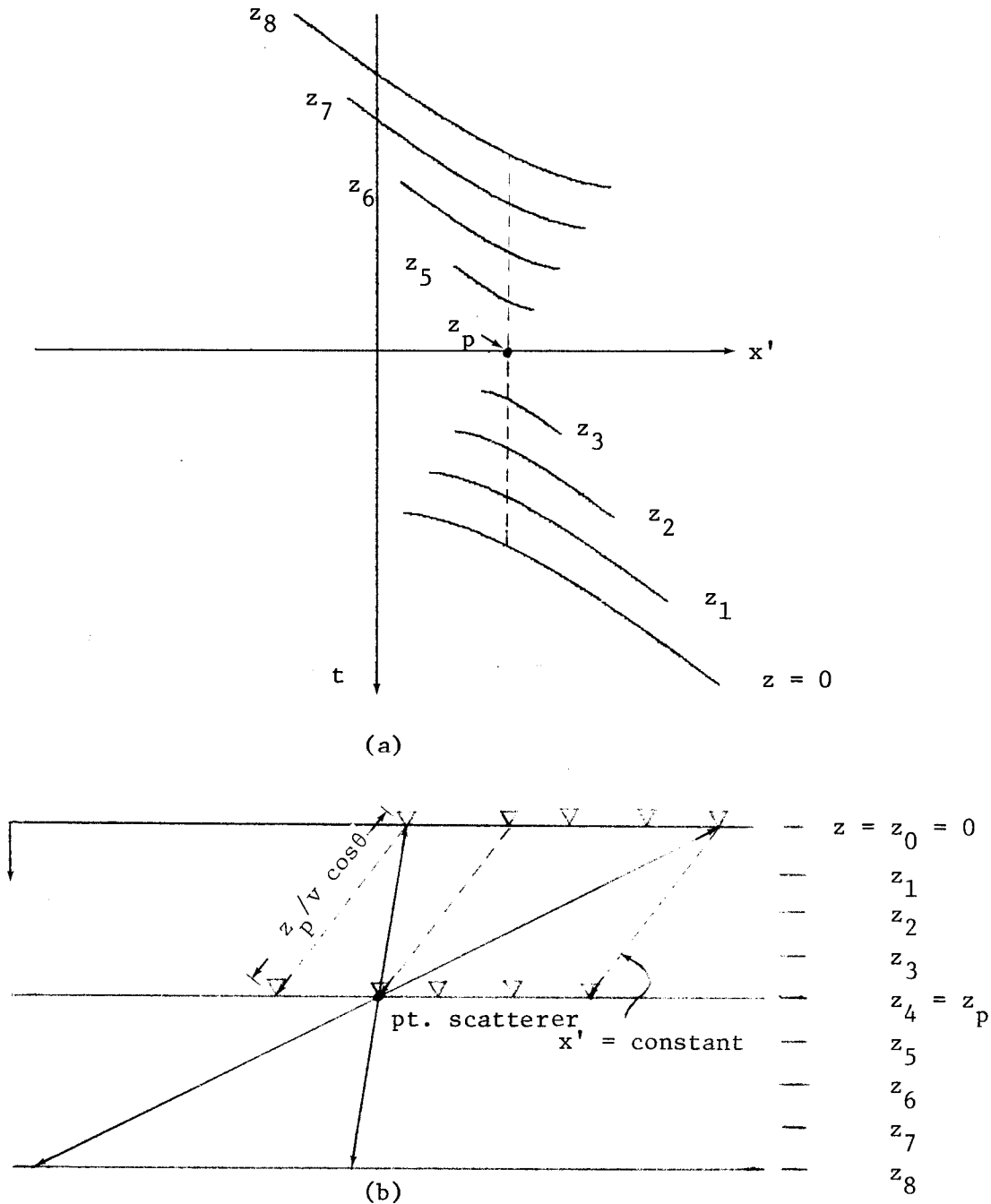


FIGURE 5.—Slanted downward continuation of receivers. The direction of downward continuation is shown by the dashed lines in (b). The travel time curves in (a) are plotted in x', t space, where x' ($= x + z \tan\theta$) is constant along the slanted paths. As the receivers are downward continued, energy migrates towards a point on the flank of the original surface hyperbola, corresponding to $x' = x_0'$ (vertical dashed line). The hyperbolic tails in the lower and upper quadrants correspond to under- and overmigrated energy, respectively. Because the direction of downward continuation splits the range of propagation angles from the point scatterer, the 15° equation can be used as the downward continuation operator. See Figs. 6(b) and 6(c) for more information.

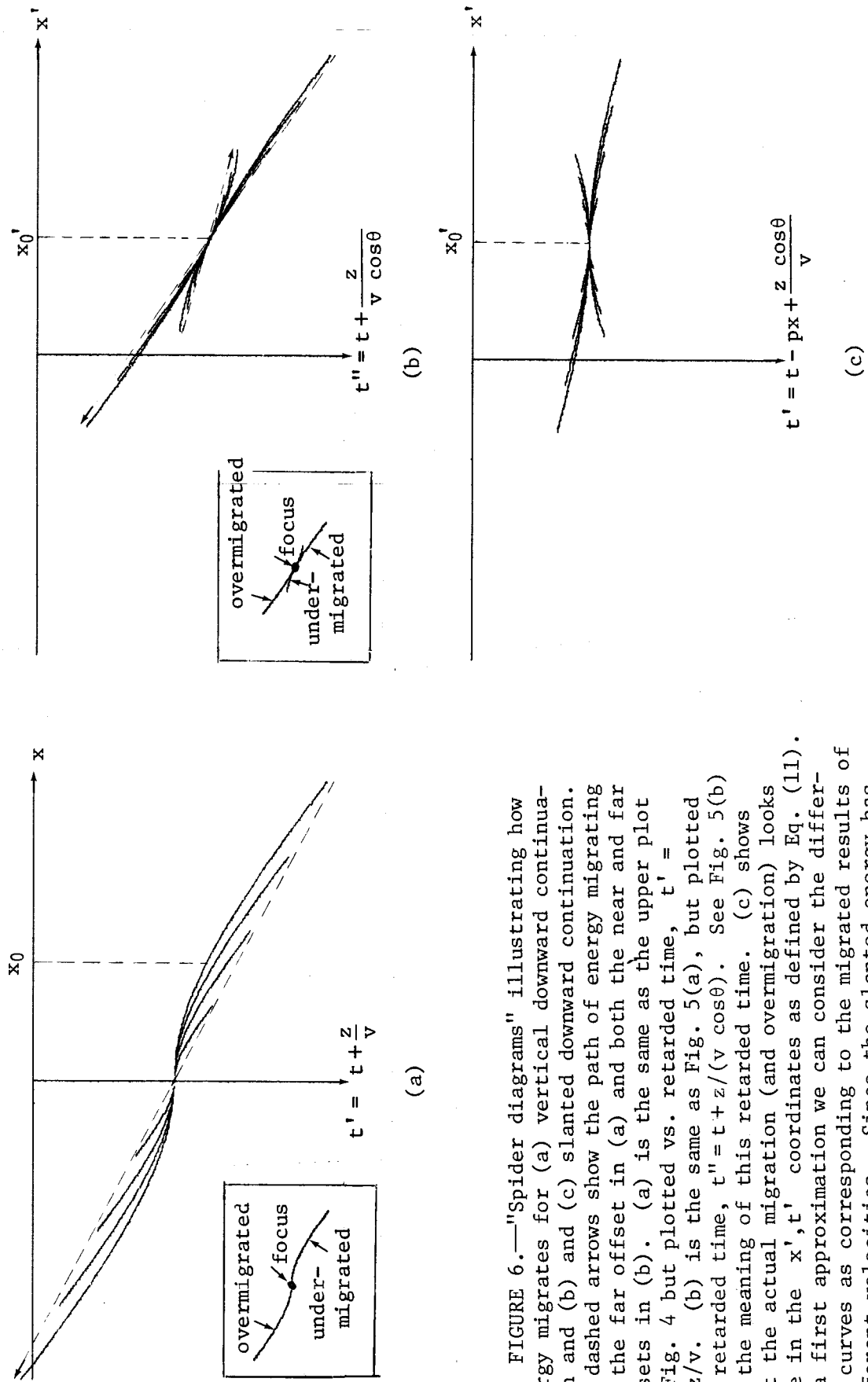


FIGURE 6.—"Spider diagrams" illustrating how energy migrates for (a) vertical downward continuation and (b) and (c) slanted downward continuation. The dashed arrows show the path of energy migrating for the far offset in (a) and both the near and far offsets in (b). (a) is the same as the upper plot in Fig. 4 but plotted vs. retarded time, $t' = t + z/v$. (b) is the same as Fig. 5(a), but plotted vs. retarded time, $t'' = t + z/(v \cos \theta)$. See Fig. 5(b) for the meaning of this retarded time. (c) shows what the actual migration (and overmigration) looks like in the x', t' coordinates as defined by Eq. (11). To a first approximation we can consider the different curves as corresponding to the migrated results of different velocities. Since the slanted energy has less distance to migrate it is less susceptible to velocity errors. The insets in (a) and (b) show an equivalent amount of under- and overmigration and indicate that the slanted downward continuation is much more tolerable to velocity errors.

$t'' = t + z/(v \cos\theta)$. The $\cos^{-1}\theta$ factor in the latter case accounts for the added travel time to get to a certain depth via a slanted path as opposed to a vertical path [see Fig. 5(b)]. The dashed arrows in these figures show the path in (x, t') and (x', t'') space that energy follows as the receivers are continued downward. In the case of vertical downward continuation, 6(a), the energy migrates from the outer to inner trace and focuses at $x=0$. If an incorrect velocity is chosen to do the migration, then the hyperbola will either not collapse totally or will collapse beyond the focus corresponding to the undermigrated and overmigrated cases shown in the inset in 6(a). In the case of slanted downward continuation, energy migrates from both the near and far offsets towards a central focus point on the hyperbola. The inset in 6(b) shows the analogous result of under- and overmigration in the slanted frame. A comparison of the insets in 6(a) and 6(b) indicate that the slanted downward continuation is much more tolerant to velocity errors than the vertical downward continuation.

Figure 6(c) shows the hyperbolas as they appear in the actual (x', t') space (defined below) during the downward continuation. The focus in this coordinate system is the top of the skewed hyperbola as shown in Fig. 3.

Combining the ideas of linear moveout and slanted directions of downward continuation, we write the following stratified media coordinate transformation

$$\begin{aligned} x' &= x + \int_0^z \tan\theta(z) dz, \\ z' &= z, \\ t' &= t - px + \int_0^z \frac{\cos\theta(z) dz}{v(z)}. \end{aligned} \quad (11)$$

Note that no knowledge of velocity is needed to transform the surface data into the slanted system.

The Jacobian for the coordinate transformation (11) is

$$\begin{bmatrix} t'_t & t'_x & t'_z \\ x'_t & x'_x & x'_z \\ z'_t & z'_x & z'_z \end{bmatrix} = \begin{bmatrix} 1 & -p & v^{-1}\cos\theta \\ 0 & 1 & \tan\theta \\ 0 & 0 & 1 \end{bmatrix}. \quad (12)$$

The invariance of wavefields implies $P(x,z,t) = Q(x',z',t')$. Taking the appropriate partial derivatives and substituting into $P_{xx} + P_{zz} = (1/v^2)P_{tt}$,

$$\left[(-p\partial_{t'} + \partial_{x'})^2 + \left(\frac{\cos\theta}{v} \partial_{t'} + \tan\theta \partial_{x'} + \partial_{z'} \right)^2 - \frac{1}{v^2} \partial_{t't'} \right] Q = 0.$$

The coefficients of the $\partial_{t't'}$ and $\partial_{x't'}$ terms vanish identically, and the remaining terms leave

$$(1 + \tan^2\theta)Q_{x'x'} + \frac{2\cos\theta}{v} Q_{z't'} + Q_{z'z'} + 2\tan\theta Q_{x'z'} = 0. \quad (13)$$

We now assume that the Fresnel approximation is valid and drop the last two terms, leaving

$$Q_{z't'} = - \frac{v}{2\cos^3\theta} Q_{x'x'}. \quad (14)$$

Dropping the $Q_{x'z'}$ term in (13) means that the skewed hyperbolas in the slanted coordinate system will be treated as if they were true hyperbolas.

Equation (14) is simply the 15° equation with the velocity weighted by an inverse $\cos^3\theta$. Defining a new coordinate

$$d' = \int_0^z \frac{v}{\cos^3\theta} dz \quad (15)$$

enables us to write a velocity-independent 15° equation as before,

$$Q_{d't'} = - \frac{1}{2} Q_{x'x'}. \quad (16)$$

In the slanted coordinate system defined by Eq. (11), we expect that the 15° wave equation can be used as the wave operator to downward continue the common shot and common geophone gathers. Consequently, we can make the downward continuation step velocity independent. Once the velocity has been estimated down to some level, the corresponding wavefield at that level can be found by simply transforming back into real earth space and time coordinates. Our next step will be to set up an operational procedure of velocity estimation based

on slanted downward continuation using Eq. (16) and the transformation (11). The velocity estimates will be based on the locations, in (x',t') space, of the tops of the skewed hyperbolas. Since the downward continuation is velocity independent, the migrated section will be readily obtainable by transforming the gathers back to real earth coordinates and using the zero-offset traces.

References

- [1] Schultz, P. S. and Claerbout, J. F. (1976), "Estimation of lateral velocity variation, Abstract," paper presented at the 46th annual meeting of SEG, October 1976.
- [2] Schultz, P. S., *Velocity estimation by wavefront synthesis*, Ph.D. thesis, Stanford University, 1976; also, SEP-9.
- [3] Claerbout, J. F., "How to measure rms velocity with a straightedge and ruler, " SEP-11.
- [4] Claerbout, J. F., "Migration in media with strong lateral velocity variation," SEP-8, pp. 1-7.